Supplementary Figure 1

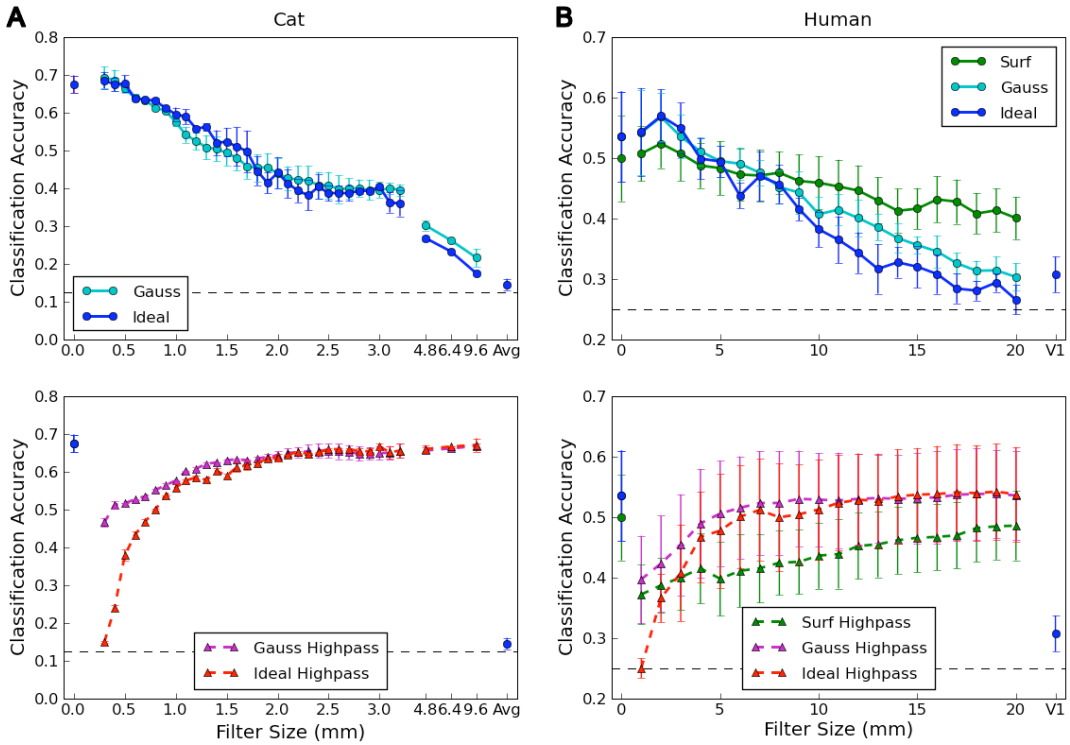

Supplementary Figure 1. Comparison of effects of different filter types on orientation classification accuracy. (**a**) Gaussian and ideal filters had similar effects on the lowpassed cat data, but performance diverged at small filter sizes in the highpassed cat data. Gaussian filters do not isolate the desired spatial frequencies as precisely as do ideal filters, with patterns on scales outside the desired range of frequencies being attenuated, but not eliminated. The fine-scale Gaussian highpass data therefore includes substantial contributions from coarse-scale patterns, which are absent in the corresponding ideal filter data. (**b**) The human data was analyzed by Gaussian and ideal 3D volumetric filters, as well as a 2D iterative cortical surface-based smoothing method (Hagler et al., 2006). As with the cat data, the volumetric ideal and Gaussian filters had similar effects on classification accuracy, except at fine spatial scales close to the 1mm voxel size. Gaussian lowpassed data also showed modestly better performance than the ideal lowpassed data, possibly again due to the comparatively poor

frequency isolation of Gaussian filters. Surface-based smoothing, which includes only voxels identified as grey matter, leads to a more gradual decline in accuracy with increasing lowpass filter size, and a more gradual rise in accuracy for the complementary highpassed images. Performance remains well above chance even with 20mm of surface-based smoothing, the most computationally feasible with the iterative averaging method used here.

Supplementary Figure 2

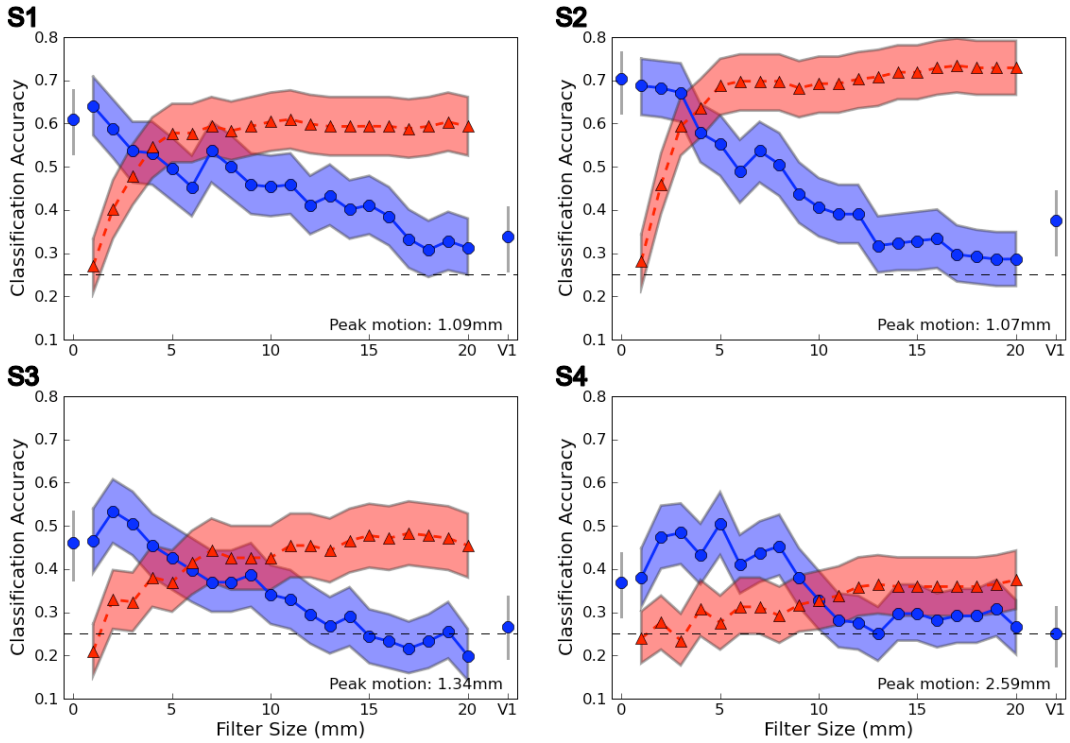

Supplementary Figure 2. Orientation classification for individual human subjects (**S1-S4**). Although classification accuracy of the original, unfiltered fMRI images varied widely between subjects, 3 of 4 showed similar patterns of continuous declining accuracy with increasing lowpass filtering (**S1-S3**). The remaining subject (**S4**) showed a slight rise in classification accuracy with 2-8mm of smoothing, but also exhibited nearly twice the amount of motion during the scan session as any other subject. Shading indicates 95% binomial confidence intervals based on 192 (**S1,S2,S4**) or 176 (**S3**) blocks of classified orientation data, half from each hemisphere.

Supplementary Figure 3

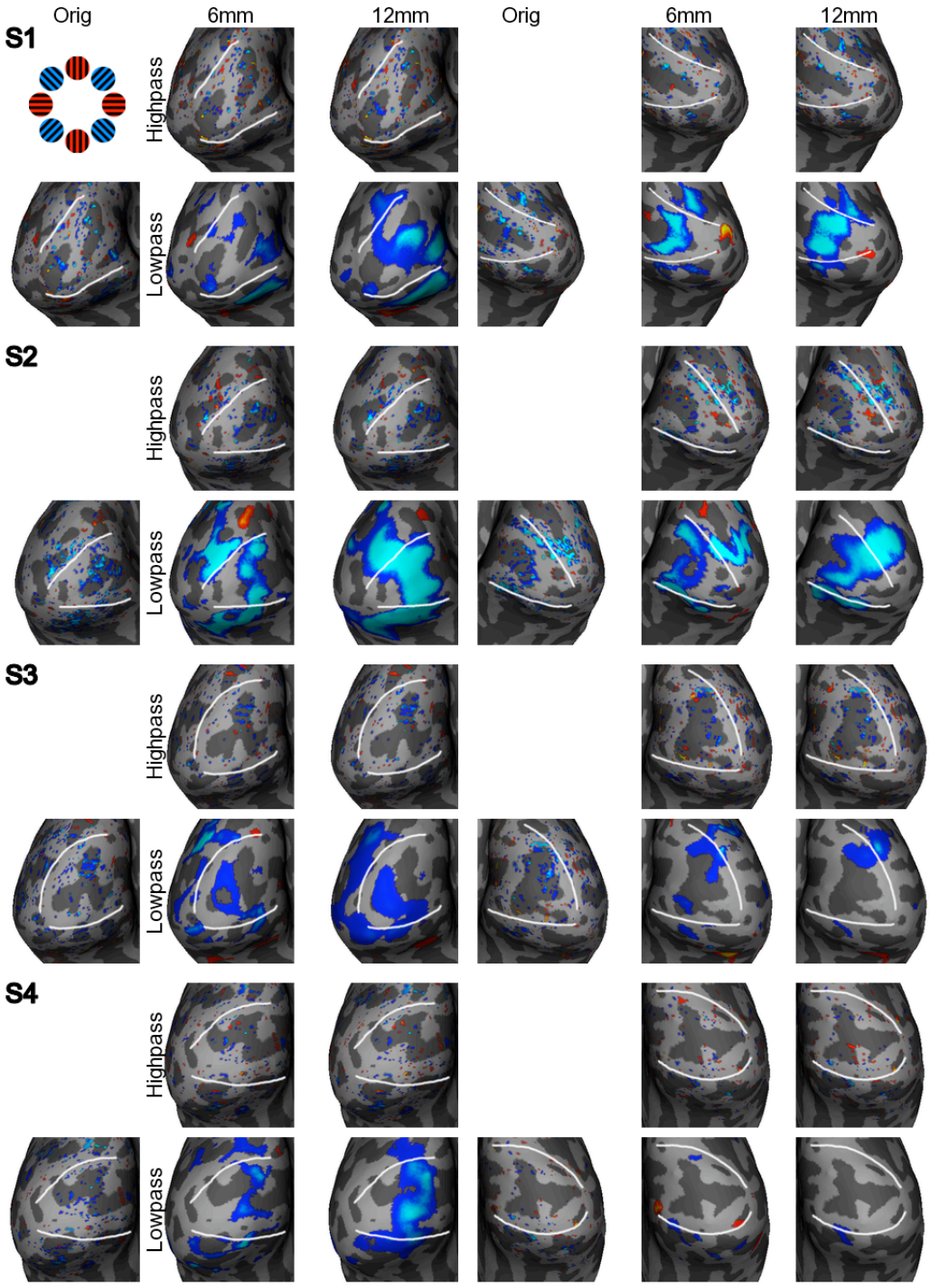

Supplementary Figure 3. Oblique effect in individual subjects (**S1-S4**). Color scale shows the contrast of cardinal (red) versus oblique (blue) orientations in the contralateral visual hemifield. In a majority of hemispheres, greater

responses are found to oblique orientations, most clearly seen in the lowpassed data. The complementary highpassed data shows comparatively weak responses in most hemispheres. White lines show the borders of retinotopically-identified V1. Statistical maps are thresholded at a minimum level of $P < 0.05$ (uncorrected) and a maximum level of $P < 0.001$ (uncorrected), to be sensitive to weak effects.

Supplementary Figure 4

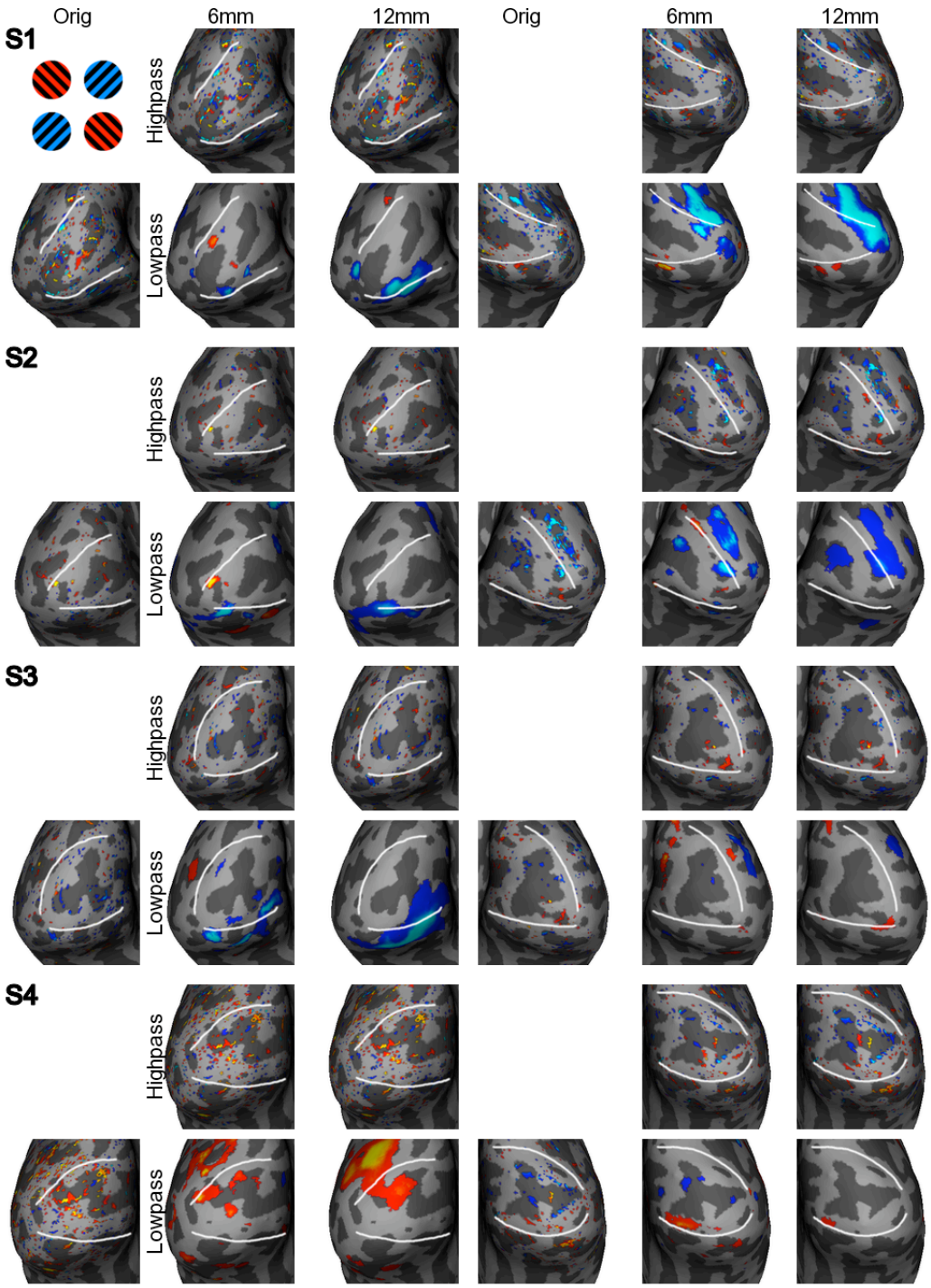

Supplementary Figure 4. Radial bias in individual subjects (**S1-S4**). Color scale shows the contrast of 135° (red) versus 45° (blue) orientations. A radial

bias effect is expected to result in preferential responses to 135° orientations in left dorsal and right ventral visual cortex, and to 45° in left ventral and right dorsal visual cortex (Sasaki et al., 2006). Activation consistent with this is observed in many hemispheres, most clearly in the lowpassed data. Radial bias effects are not evident in the complementary highpassed data. Statistical maps are thresholded at a minimum level of $P < 0.05$ (uncorrected) and a maximum level of $P < 0.001$ (uncorrected), to be sensitive to weak effects.

Supplementary Figure 5

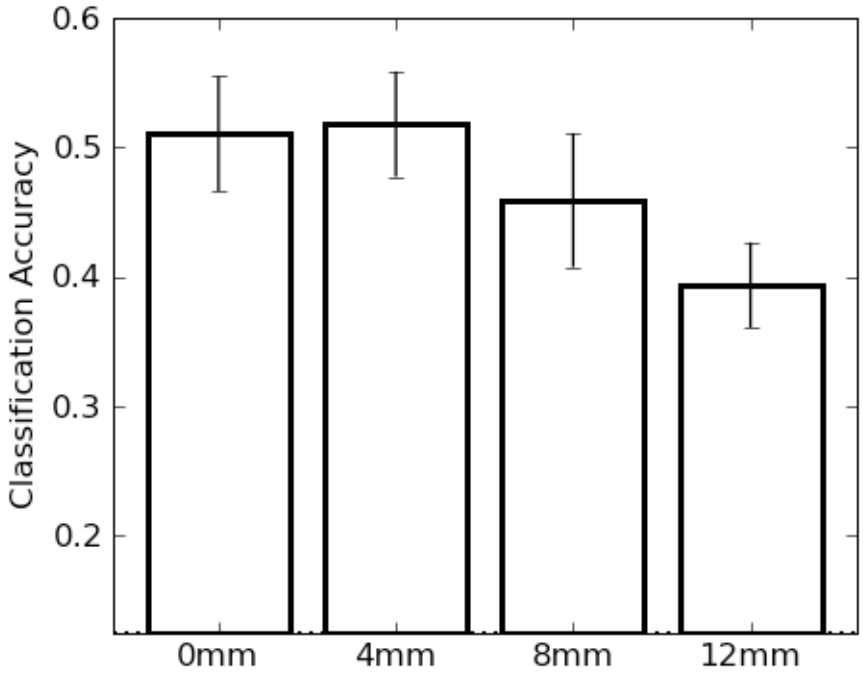

Supplementary Figure 5. Reanalysis of the orientation data of Kamitani & Tong (2005), acquired at 3mm resolution, with increasing levels of smoothing. Performance is significantly degraded (relative to the original images) at 8mm (one tailed paired t[3]=2.55, *P* = 0.042) and 12mm (t[3]=3.57, *P* = 0.019) FWHM Gaussian smoothing. Smoothing by a fixed amount is expected to have a proportionately smaller impact on lower-resolution data.

Supplementary Figure 6

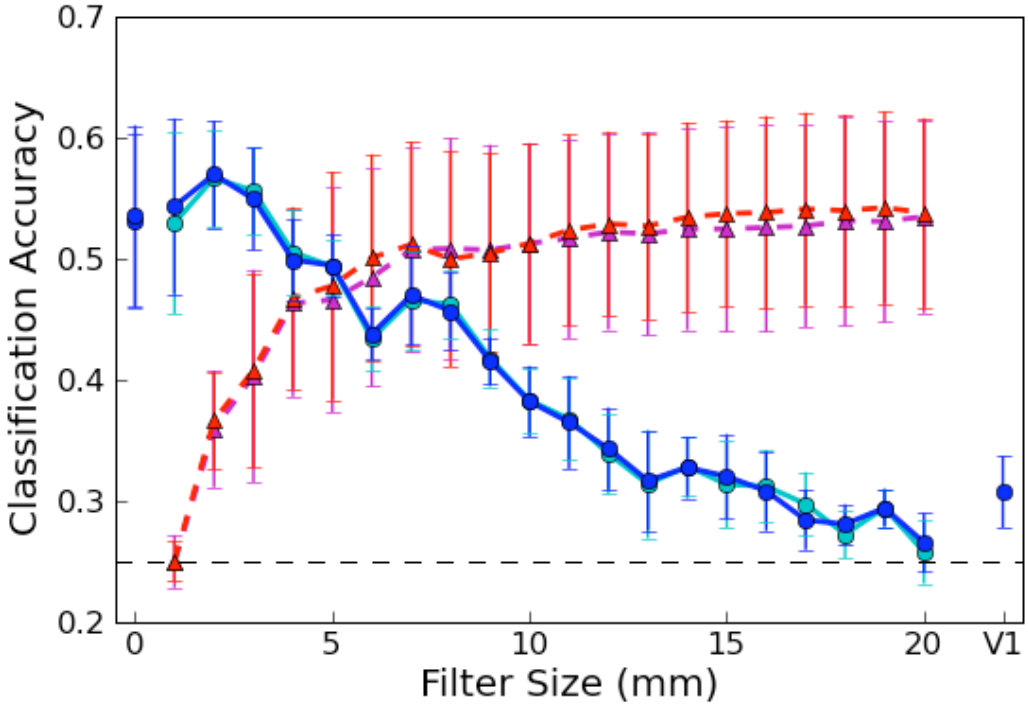

Supplementary Figure 6. Comparison of classification accuracy with and without cross-validated feature selection. For the multiscale pattern analyses reported in the main text, we selected visually active voxels based on a contrast of all orientations versus fixation ($P < 0.010$) using only those N-1 functional runs that comprised the current classification training set (blue and red curves from **Fig. 2**). However, we obtained almost identical results when visually active voxels were selected based on all N runs (purple and cyan lines), despite concerns that have been raised as to whether this procedure could represent a form of statistical "double-dipping" (e.g., Kriegeskorte et al., 2009). Because the contrast used to select visually active voxels is orthogonal to the categories being classified (i.e., orientation), we expected negligible levels of statistical bias to emerge from a voxel-selection procedure involving all N runs.